arXiv:astro-ph/0412606v1 22 Dec 2004

Constraining the local radiation field and the grain size distribution in dust SED modelling of dwarf galaxies

Frédéric GALLIANO

SAp, CEA/Saclay, l'Orme des Merisiers, 91191 Gif, France
Infrared Astrophysics branch, code 685, NASA GSFC, Greenbelt MD 20771, USA

Abstract. I present a simple self-consistent dust spectral energy distribution (SED) model that has been applied to fit the well-sampled observed UV-to-radio SED of four nearby starbursting dwarf galaxies. The main originality of this model is that numerous multi-wavelength observations, from UV to millimeter (mm), constrain in a self-consistent manner, both the local radiation field and the grain size distribution. I finally present the results of our model and discuss the average dust properties in these dwarf galaxies.

INTRODUCTION: THE DIFFICULTIES TO INTERPRET AN OBSERVED DUST SED

Most of the current dust models [1, 2, 3, 4] have been developed to describe the emission from the diffuse Galactic ISM. Consequently, their application to other galaxies is not straightforward.

First, the dust abundances and grain size distribution are likely to depend significantly on the local physical conditions. Indeed, the grains can undergo coagulation and accretion of material in dense media; fragmentation and erosion in diffuse shocked media; evaporation of smaller grains in H II regions and injection of newly-formed grains by evolved stars and supernovae. Second, the interpretation of an observed IR-to-millimeter SED of a galaxy in terms of dust properties (composition, mass, size distribution) is difficult due to the fact that the hardness and intensity of the local interstellar radiation field (ISRF) vary strongly from quiescent to starforming regions. This ISRF being the heating source of the dust, its spectral shape and intensity have a direct effect on the spectrum emitted by the dust.

Figure 1 illustrates the degeneracy between the effects of the ISRF and those of the size distribution. The two top plots show an observed dust SED (the grey crosses; these fluxes are identical in the two plots). They have been fitted with the Désert et al. [1] model (hereafter DBP90), by varying two different sets of parameters: *(i)* the top-left plot has been fitted by varying the ISRF and keeping the Galactic size distribution *(ii)* the top-right plot has been fitted by varying the size distribution and keeping the Galactic ISRF. The bottom-left plot shows the radiation field required to produce the top-left plot, compared to the Galactic one. This ISRF is harder and more intense, thus the grains are hotter, emitting at shorter wavelengths. The bottom-right plot shows the size distribution

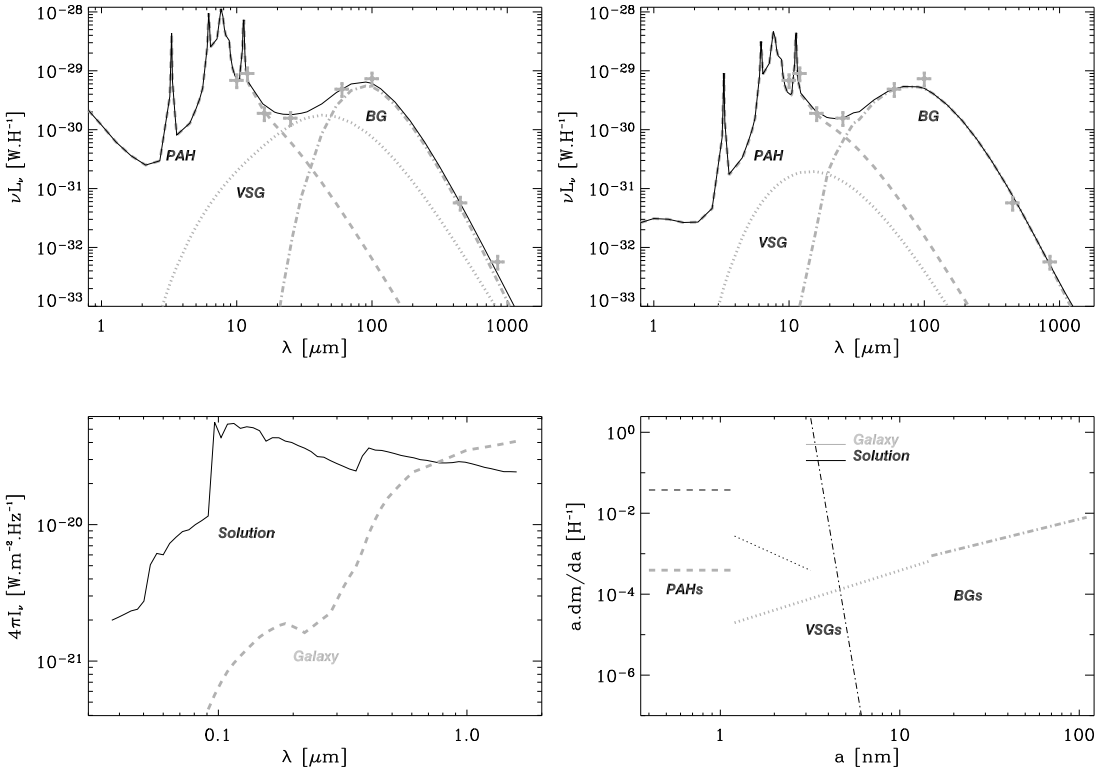

FIGURE 1. Demonstration of the degeneracy in dust SED modelling. The model used to fit these SEDs is the Désert et al. [1] model. The three dust components are the PAHs (polycyclic aromatic hydrocarbons), the VSGs (very small grains) and the BGs (big grains). The grain radius is a, and dm/da is the mass of grains between a and $a+da$. From Galliano et al. [5].

required for the top-right plot, compared to the Galactic one. To fit this SED with a soft and low ISRF, we need to increase the abundance of small grains which are the hottest ones.

These figures emphasize the necessity to constrain independently both the ISRF and the grain size distribution when modelling a dust SED.

THE CHOICE OF A SIMPLE SELF-CONSISTENT MODEL

The multiwavelength observations

We have built the observed UV-to-radio SED of four nearby starburst dwarf galaxies (NGC 1140, NGC 1569, II Zw 40 and He 2-10) by collecting data from the literature together with our mid-IR ISOCAM and submm SCUBA (Figure 2) and MAMBO observations. The broadband fluxes constrain the stellar continuum, the dust emission and the free-free/synchrotron contribution. The mid-IR ionic lines observed by ISOCAM are used to constrain the ionized gas properties, and the CO line measurements are used

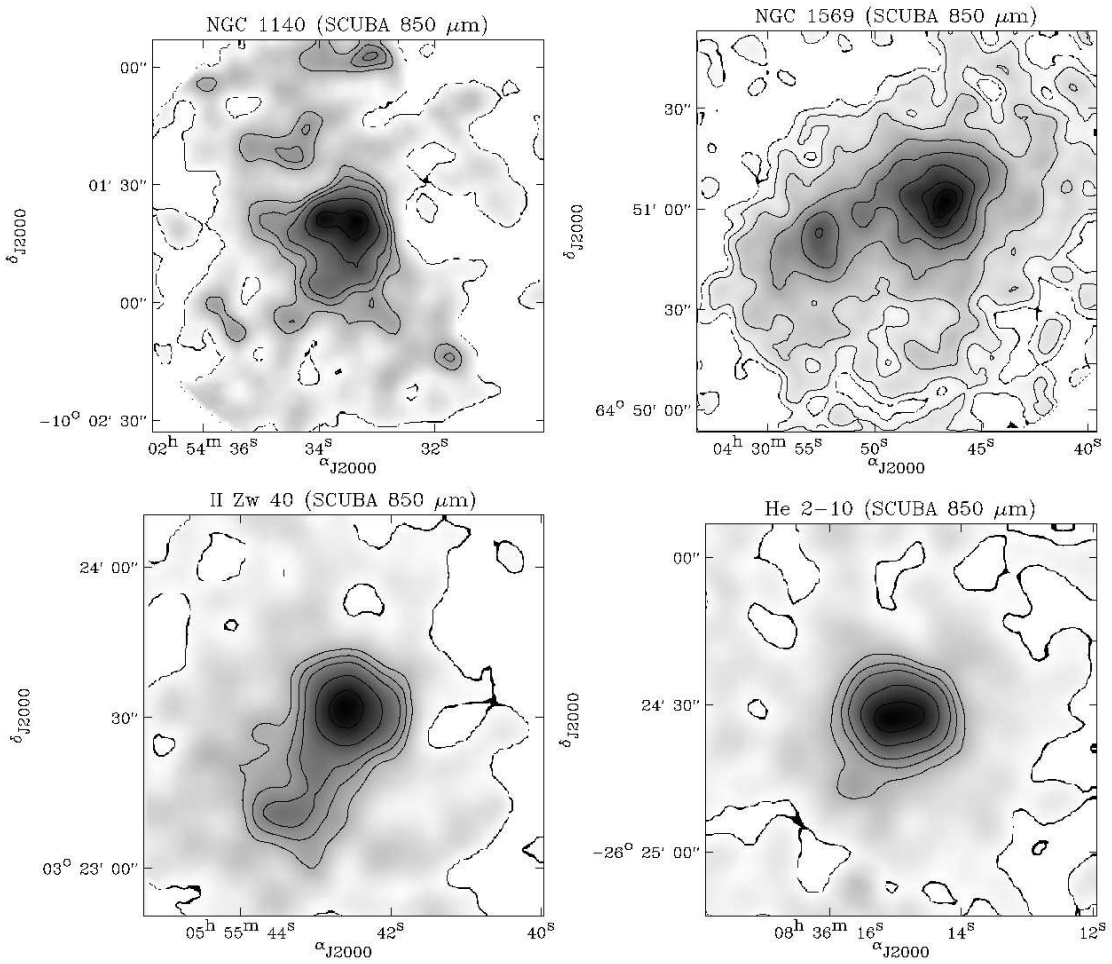

FIGURE 2. 850μm SCUBA images of the four dwarf galaxies. From Galliano et al. [6] and Galliano et al. [5].

to remove the molecular gas contribution to the submillimeter broadbands.

The model

The strategy we adopted to model the dust SED of these four nearby dwarf galaxies is motivated by the degeneracy shown in Figure 1. The different steps are the following.

1. An ISRF is synthesized using PÉGASE [7]. We consider two age populations: one accounting for the old underlying stars and a young one accounting for the stars formed during the recent starburst. This ISRF fits the unreddened UV-optical broadband fluxes. The mean internal optical depth is computed from the energy balance between the IR-mm emission and the UV-optical absorption. The young stellar population is not well constrained since we lack UV data (at shorter wavelengths than U band).

2. The ratio of the mid-IR ionic lines ([Ne III] $\lambda 15.56\,\mu$m, [Ne II] $\lambda 12.81\,\mu$m, [S IV] $\lambda 10.51\,\mu$m) observed by ISOCAM are very sensitive to the hardness of the radiation field and are not significantly affected by extinction. The uncertainty of the UV part of the ISRF is removed by constraining the photoionisation model CLOUDY [8] by these mid-IR ionic line ratios.
3. The synthesized ISRF is used as the heating source of the DBP90 dust model. We vary the grain size distribution in order to fit the IR-mm emission. The dust properties deduced from this fit allow us to synthesize an average extinction curve for each galaxy.
4. This extinction curve is used to unredden the UV-optical observations. We iterate these four steps until we reach an agreement between extinction and emission properties.

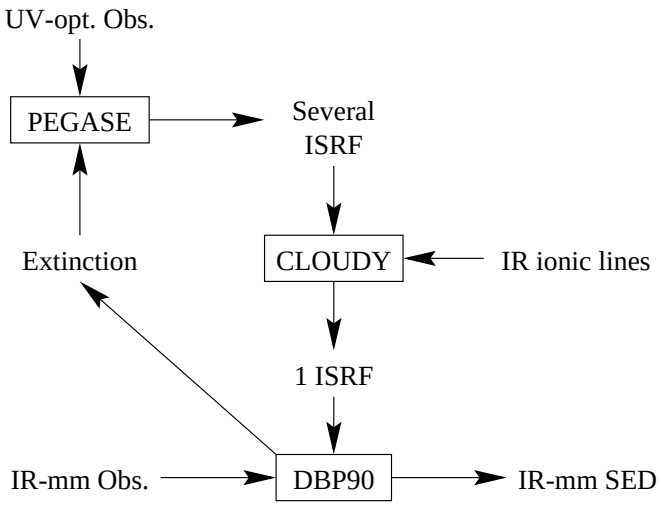

FIGURE 3. General method used to fit the SEDs of the four dwarf galaxies [6, 5].

Figure 3 summarizes the different steps of our modelling. This method allow us to independently constrain the local ISRF and the average size distribution in a self-consistent way, taking into account the emission and extinction properties of the dust.

AVERAGE DUST PROPERTIES IN FOUR STARBURSTING DWARF GALAXIES

Figure 4 shows the global SEDs of our four galaxies. The IR-mm part, emitted by the dust is hotter than in the Milky Way. There remain a submillimeter emission excess in each of the SEDs that we cannot explain with regular dust properties or radio-molecular contributions. In the next section, I will present the modeled dust properties. Then, I will discuss the consequences of this submillimeter excess.

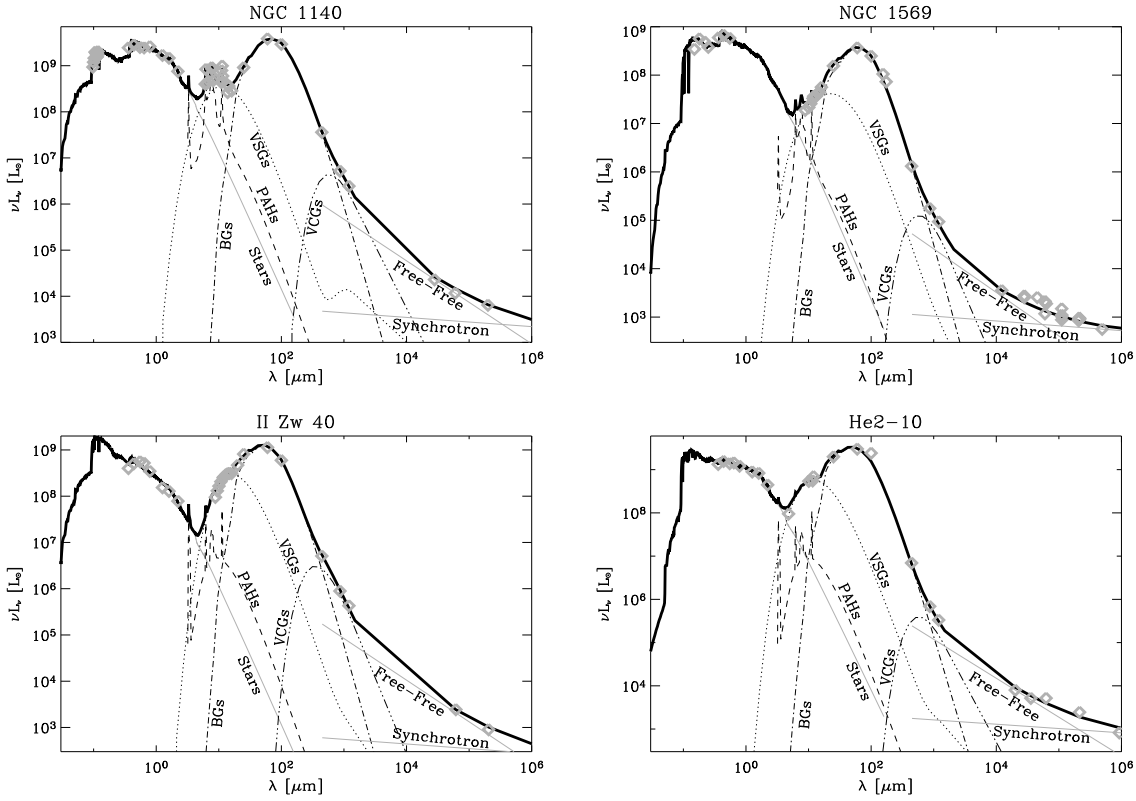

FIGURE 4. Multiwavelength observed and modelled global SEDs of four dwarf galaxies [6, 5]. The grey diamonds are the observations and the lines are the model.

The modeled dust properties

We first notice that the PAHs are underabundant in these galaxies. They are very weak in NGC 1569, II Zw 40 and He 2-10. Only NGC 1140, which is the most quiescent of these objects, present some relatively strong mid-IR band emission [9].

Second, the silicate and graphite size distributions constrained by the fit of the dust SED are different from those of the Galaxy. The grains are on average smaller ($\sim 3-4$ nm) than those in the Milky Way. Figure 5 shows the size distribution of NGC 1569 compared to the Galactic size distribution before and after a shock [10]. The grain size segregation is consistent with the erosion and the fragmentation of the grains by the numerous supernovae shock waves that these galaxies have recently experienced.

A consequence of this small average grain size is that the bulk of the dust emission originates into stochastically heated particles. Another consequence is that the synthesized extinction curves are qualitatively similar to those observed toward several lines of sight in the Magellanic Clouds. Their slope is almost linear in $1/\lambda$ and they have a lower extinction bump, except in one galaxy (figure 6).

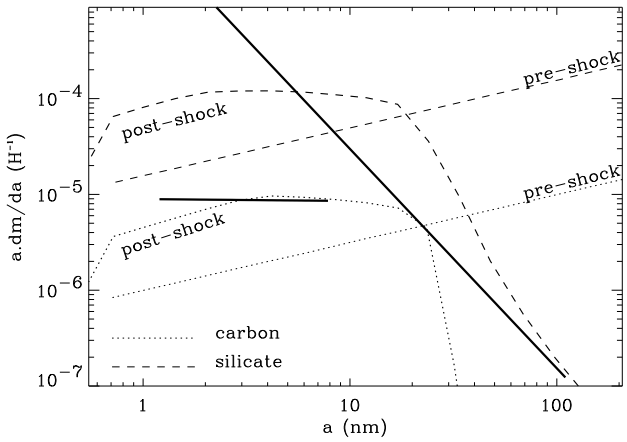

FIGURE 5. Grain size distribution for NGC 1569 compared to a graphite and silicate size distribution before (distribution of [11]) and after a shock wave [10]. From Galliano et al. [6].

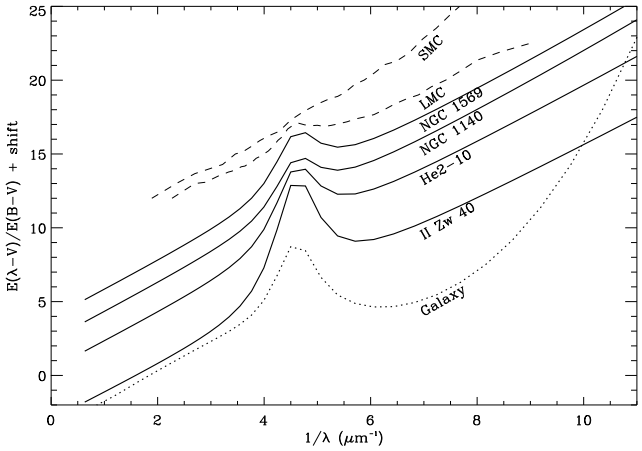

FIGURE 6. Synthesized extinction curves for our four galaxies compared to the Galactic and the Magellanic extinction curves. These curves have been shifted for clarity. From Galliano et al. [5].

The submillimeter excess

The submillimeter excess could be either due to peculiar grain optical properties or to a component of very cold dust. Laboratory data show that the emissivity index drops at low temperature [12, 13]. However, these data can not account for this excess, since the actual change in the slope occurs at a longer wavelength [6].

Thus, we explore the second hypothesis which is fully quantifiable. The temperatures required to fit the excess are low ($T \simeq 5-9\,\mathrm{K}$). The dust mass deduced from this component is a large fraction of the total dust mass ($40-80\,\%$). A detailed treatment [6, 5] shows that this very cold grain (VCG) hypothesis is consistent with very small and dense clumps. Figure 7 shows the structure of such a clump. The very cold dust is

embedded and heated only by the IR radiation.

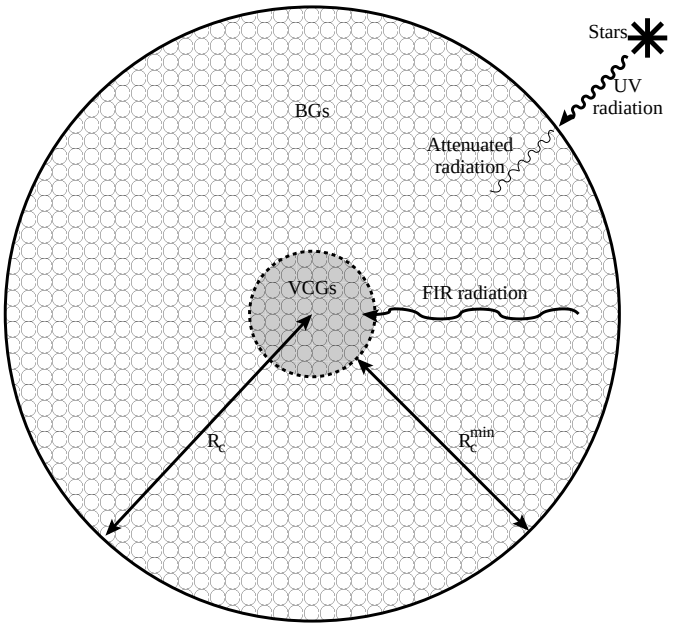

FIGURE 7. Structure of a clump consistent with the very cold dust hypothesis. From Galliano et al. [6].

PROSPECTIVES

This modelling was a first step to investigate the detailed dust properties in low-metallicity environments. A further improvement would be to take into account the geometry of the environment, by using the spatial information that we have on these galaxies, and treating the radiative transfer.

The second extension of this study would be to consider a larger sample in order to disentangle the effects of the low-metallicity of the medium and the effects of the radiation field. The knowledge of galaxy SEDs is very important to prepare the future missions like Herschel.

ACKNOWLEDGMENTS

This presentation was performed while the author held a National Research Council Research Associateship Award at NASA GSFC.

REFERENCES

1. Désert, F.-X., Boulanger, F., and Puget, J.-L., *A&A*, **237**, 215–236 (1990).
2. Li, A., and Draine, B. T., *ApJ*, **554**, 778–802 (2001).
3. Draine, B. T., and Li, A., *ApJ*, **551**, 807–824 (2001).

4. Zubko, V., Dwek, E., and Arendt, R. G., *ApJS*, **152**, 211–249 (2004).
5. Galliano, F., Madden, S. C., Jones, A. P., Wilson, C. D., and Bernard, J.-P., *A&A*, *submitted* (2004).
6. Galliano, F., Madden, S. C., Jones, A. P., Wilson, C. D., Bernard, J.-P., and Le Peintre, F., *A&A*, **407**, 159–176 (2003).
7. Fioc, M., and Rocca-Volmerange, B., *A&A*, **326**, 950–962 (1997).
8. Ferland, G. J., Hazy, a brief introduction to cloudy, Tech. rep., University of Kentucky, department of physics and astronomy (1996).
9. Madden, S. C., Galliano, F., Jones, A. P., and Sauvage, M., *A&A*, *to be submitted* (2004).
10. Jones, A. P., Tielens, A. G. G. M., and Hollenbach, D. J., *ApJ*, **469**, 740–764 (1996).
11. Mathis, J. S., Rumpl, W., and Nordsieck, K. H., *ApJ*, **217**, 425–433 (1977).
12. Agladze, N. I., Sievers, A. J., Jones, S. A., Burlitch, J. M., and Beckwith, S. V. W., *ApJ*, **462**, 1026–1040 (1996).
13. Mennella, V., Brucato, J. R., Colangeli, L., Palumbo, P., Rotundi, A., and Bussoletti, E., *ApJ*, **496**, 1058–1066 (1998).